

Calculation of Dynamic Amplification Factor for Railway Concrete and Masonry Arch Bridges Subjected to High-speed Trains

Peyman Azimi¹, Mahdi Yazdani^{1*}

¹ Department of Civil Engineering, Faculty of Engineering, Arak University, Arak, P.O. B. 38158–879, Iran

* Corresponding author, e-mail: m-yazdani@araku.ac.ir

Received: 06 November 2021, Accepted: 05 April 2022, Published online: 16 May 2022

Abstract

The dynamic amplification factor (DAF) is one of the most important parameters to express the dynamic behavior of bridges under moving loads. This parameter is used in bridge design codes instead of exhaustive dynamic analyses. Therefore, the DAF and the possible derived relationships can be good alternatives to dynamic analyses because of time and computational cost savings. Masonry arch bridges are complex infrastructures due to their geometry and structural behavior, and it is troublesome to prepare an accurate numerical model. To conduct dynamic analyses, due to their multiplicity, calculating the DAF of the bridges imposed by high-speed trains can lead to a rapid assessment of these old railway arch bridges. For this purpose, in the present study, the finite element models of two concrete and masonry arch bridges with small fill material heights, which are completely different in terms of geometric and mechanical characteristics, were prepared. In the next step, by performing 378 dynamic analyses based on the 27 different train models, the DAF has been computed. The results show that the calculated DAFs are in the rational range, and bogies interval, axles interval, and span length are recognized as the most important parameters in the DAF changes.

Keywords

old railway infrastructures, concrete and masonry arch bridges, dynamic amplification factor, high-speed trains, finite element models

1 Introduction

Masonry arch bridges are one of the most vital structures of Iran's railway network since there are about 3300 masonry arch bridges out of 30000 railway bridges. Many of these railway bridges still in service have been designed back when vehicles' speeds were considerably lower as these structures have a history extending back about 90 years. At present, the masonry arch bridges in Iranian railway network are being serviced for trains with a maximum speed of 80 km/h. Design calculations for nearly all masonry arch bridges were based on simplified analysis considering service loads of that time (low-speed trains). The demand for transportation is generally influenced by factors such as time considerations as the main factor that determines whether or not people choose a certain mode of transportation. As transportation systems have developed over time, the speed and performance of these systems have improved drastically. The development of railway networks for high-speed trains is rapidly growing in many countries around the world, to meet the increasing

demand for faster transportation. Because of the importance of passenger and freight moving time and increasing the speed of railways, the study of dynamic loads subjected to high-speed trains is more important than the load due to conventional trains. In the last few decades, the use of high-speed trains has greatly expanded all over the world which also affects Iran. Among the special considerations for high-speed railway bridges, the most relevant one is the limitation of dynamic effects when high-speed trains cross. The dynamic effect of trains on bridges is related to some important dynamic characteristics such as trains' speed. The existing masonry arch bridges cannot be replaced by any means because of time, field, and economic constraints. Hence, extensive dynamic analyses have to be taken for updating the current speed limits due to the increasing demand for railway transportation, thus maintaining the safety of the bridges [1]. So, it is necessary to evaluate the dynamic behavior of these bridges under the effect of high-speed trains.

The study of the dynamic behavior of bridges (deck bridges) imposed by moving vehicles dates back to about a century ago. Of course, the investigation of the behavior of bridges subjected to high-speed trains has been begun since the first high-speed train was used in Japan in 1964 [2]. A lot of studies have been dedicated to the investigation of the dynamic behavior of railway bridges in different types including masonry arch bridges imposed by moving trains throughout the world [3–5]. The most recent study carried out by Yazdani and Azimi [6] on masonry arch bridges under the moving high-speed trains has shown more sensitivity of the long span bridge to acceleration response notwithstanding the short span bridge to displacement response.

Although the load-carrying capacity is considered the most significant of the design criteria during the bridge design process, the dynamic behavior is also assessed by applying a parameter known as the dynamic amplification factor (DAF) to represent the bridge's dynamic characteristics. It is now well-known that all sorts of moving vehicles generate a dynamic impact effect on bridges, namely, the increment from the static load effect. Usually, they are indicated by the DAF introduced in numerous research studies and design codes. The DAF, defined as the ratio of the dynamic increment to the corresponding static response, has been used to describe the dynamic effect of moving vehicles on bridge structures [7]. The DAF is an important parameter in the design procedure of both railway and highway bridges and shall be taken into account by the evaluation of the existing bridge load-carrying capacity as well. To investigate the behavior of highway bridges under vehicles, numerous studies have been performed on determining the DAFs [8–12]. The significant role of road surface roughness in calculating DAFs, not enough evidence for a correlation between material characteristics and DAFs, and the relationship between DAFs and vehicle's speed and weight are numbers of the foremost conclusions which have been drawn [13].

DAF plays a vital role in the practice of railway bridge condition assessment. One of the most recent studies on the dynamic amplification factors (DAFs) of high-speed railway continuous bridges has revealed that the experimental formulas in the Japan Railway Technical Research Institute (JRTRI) code could make a conservative estimation of the dynamic amplification factors of high-speed railway continuous bridges [14]. Accurate evaluation of the factor will provide valuable information for enhancement railway bridges codes. A study on Korean railway steel plate girder

bridges aimed to determine the DAFs for fatigue investigation of the bridges has shown that the Korean code overestimates the DAF [15]. Furthermore, there are multiple research projects on different types of railway bridges under trains considering the DAF values [16–18]. According to these studies, different parameters affect the dynamic behavior and DAFs of bridges. Accordingly, a high impact effect has been found at shorter side spans and much lower around the longer spans in a bridge [17]. The insignificant effect of track geometry on the dynamic response of bridge [19], a regular interval of axles at the critical speeds which leads to the strong DAFs [1] and higher correlation between the rise to span ratio and the DAFs in comparison with span length and the DAFs [16] are some of the correlations between parameters. Another study that has been engaged in specifying the effects of various parameters on DAFs has shown that, however, an increase in train speed causes an increase in DAF, greater axle distance to span length ratios generate the smaller DAFs [20].

The dynamic effect has certainly sparked another worldwide debate about how to ensure the efficiency of existing bridges subjected to high-speed trains. Hence, to get a better understanding of the structural behavior of bridges under high-speed trains, and because the bridges are subjected to high impacts under loads of high-speed trains [21], it is necessary to consider the DAF. So, many authors have dealt with the DAF of bridges under high-speed trains in different countries. It has been concluded in an experimental and theoretical project which has been performed on the bridges crossed by the Korean high-speed train that, the DAFs depend on the number of coaches and the intensity of the loading [22]. As another paper's outcome it is notable that, softer ballast tends to reduce the impact response of the bridges, although the degree of reduction is only marginal [23]. The DAFs have been more affected by the increase in speed for the shortest span, whereas they remained almost constant when the velocity increased to the particular value for the longest spans [24].

In the majority of previous research conducted on the determination of DAFs of bridges, as a common part of the numerical studies, simply supported and continuous beams have been frequently used [25, 26]. On account of the inherent complexity of masonry arch bridges, no study has been reported on the DAF of masonry arch bridges from moving high-speed trains yet. This has made it increasingly important to authors to estimate the dynamic effects of high-speed trains passage on the serviceability of the existing bridge accurately.

2 Characteristics of investigated high-speed trains

In the present study, a combination of real trains along with the European standard train load models [27] designated HSLM-A and HSLM-B are imposed on railway bridges. These classifications have been intended to evaluate the dynamic behavior of the bridges applied by high-speed trains using the DAF parameters. The researchers made an effort to perform a comprehensive study of the dynamic behavior of the bridges applied by high-speed trains by extracting a thorough range of load classifications.

Some loading models are derived from real trains configuration currently in service and other loading models are proposed by European standards [27]. The loading models consist of mitigated representations in the form of different sets of concentrated loads. Real train models, types 1–10,

represent high-speed trains running on railways in the developed countries of Asia and Europe. In addition, 17 train models which are called Universal Trains comprised of two independent families identified as HSLM-A and HSLM-B.

The procedure of choosing the high-speed trains (both real trains and Universal train models) have been performed with a particular attitude towards maintaining trains' characteristics. Coach distributions, spacing of axles, and length of the train are some of the mentioned attributes in the current study. The characteristics of real high-speed trains are sorted as No. 1 to 10 and displayed in Table 1. As it is shown in Table 1, B4 and A2 are designated as the shortest and the longest trains of the HSLM category, respectively. Also, Renfe S104 and SKS are investigated as the shortest and the longest real trains, respectively.

Table 1 Characteristic of Asian, European and Universal trains

Train number	Train name	Country	Number of axles	Total length (m)	Average load of axles (kN)	Total load (kN)
Real high-speed trains						
1	RENFE S100	Spain	26	192.6	165	4290
2	RENFE S102	Spain	21	191	166	3486
3	RENFE S103	Spain	32	193.5	145	4640
4	RENFE S104	Spain	16	99.4	153	2448
5	RENFE S130	Spain	20	176.3	175	3500
6	China-Star	China	44	263	150	6600
7	KHST	Korea	46	380.2	170	7820
8	SKS	Japan	64	395	137.4	8793.6
9	TGV	France	26	193.2	168	4368
10	ICE	Germany	48	292.7	152	7296
Euro-code Standard, Type A						
11	HSLM-A1	Universal Train	50	397.4	170	8500
12	HSLM-A2	Universal Train	48	398.5	200	9600
13	HSLM-A3	Universal Train	46	397.4	180	8280
14	HSLM-A4	Universal Train	44	394.4	190	8360
15	HSLM-A5	Universal Train	42	389.4	170	7140
16	HSLM-A6	Universal Train	40	382.4	180	7200
17	HSLM-A7	Universal Train	40	397.4	190	7600
18	HSLM-A8	Universal Train	38	387.5	190	7220
19	HSLM-A9	Universal Train	36	375.4	210	7560
20	HSLM-A10	Universal Train	36	388.4	210	7560
Euro-code Standard, Type B						
21	HSLM-B1	Universal Train	8	24.5	170	1360
22	HSLM-B2	Universal Train	10	36	170	1700
23	HSLM-B3	Universal Train	15	70	170	2550
24	HSLM-B4	Universal Train	3	5	170	510
25	HSLM-B5	Universal Train	20	114	170	3400
26	HSLM-B6	Universal Train	7	19.8	170	1190
27	HSLM-B7	Universal Train	5	12	170	850

As it is depicted in Fig. 1, These 10 train models differ in total length, coach length, number of intermediate passenger coaches, axles and bogies interval, and axle loads. No. 1 to 5 are related to Spain high-speed trains (Renfe S100 to Renfe S130) [28], No. 6 refers to China high-speed

train (China Star) [29], No. 7 signifies South Korea high-speed train (KHST) [22], No. 8 symbolizes Japan high-speed train (SKS) [30], No. 9 mentions France high-speed train (TGV) [31], and No. 10 is related to Germany high-speed train (ICE) [32].

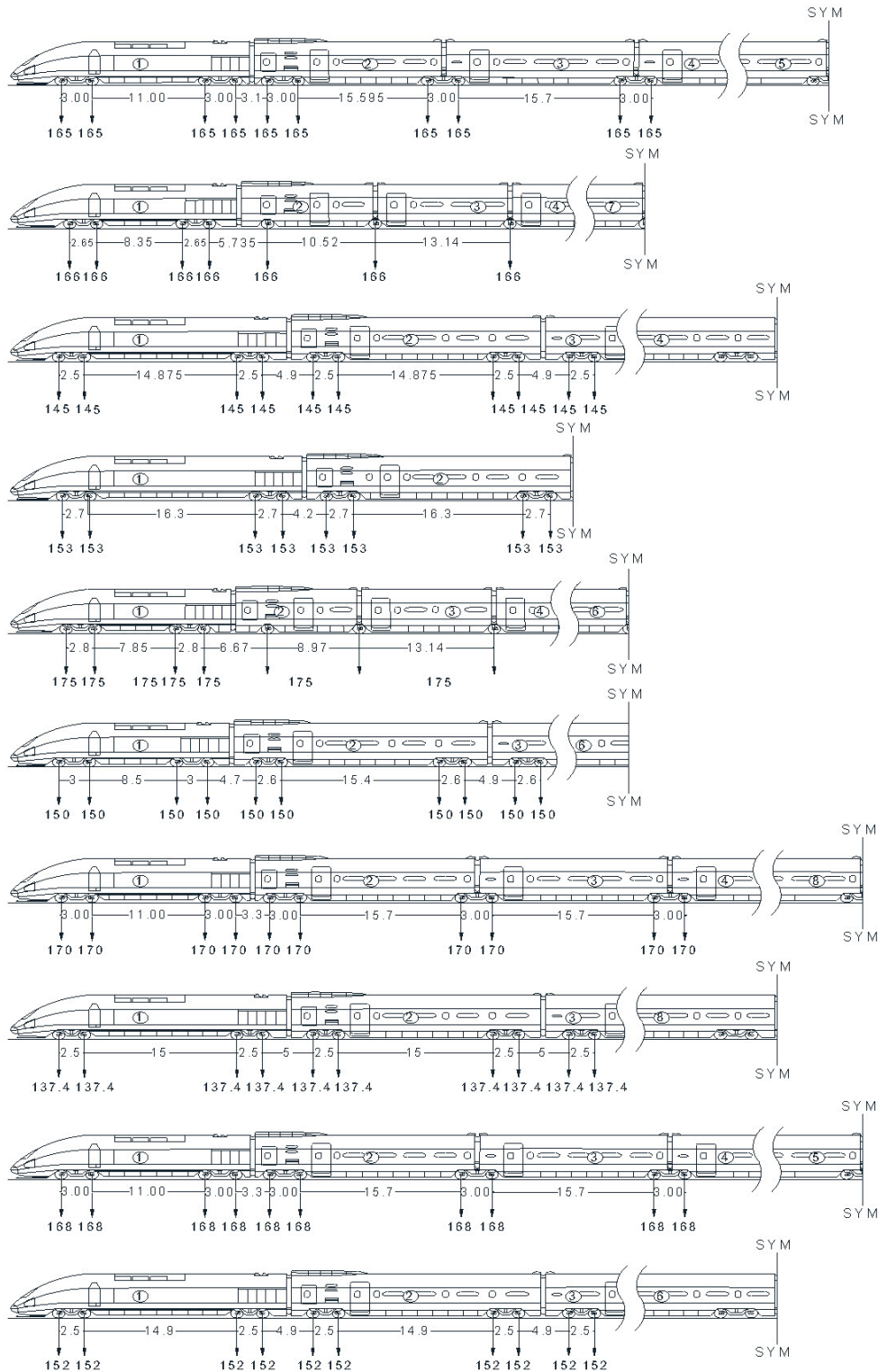


Fig. 1 Real train load models

The train load models in Eurocode are a theoretical idealization of high-speed trains. According to Eurocode, a dynamic analysis must be performed using the train load characteristic values of the high-speed HSLM load model. The HSLM consists of different train load configurations, with different characteristic axle loads and intervals between axles. These two load models also differ in coach length, the number of intermediate passenger coaches, axle spacing of bogies, and axle loads limited by the range of 170 and 210 kN. HSLM-B load models represent the concentrated loads spacing uniform axle load of 170 kN, and the number of axles is related to the bridge span length. High-speed traffic models of HSLM-A and HSLM-B represent the dynamic load effects of articulated, conventional, and regular high-speed passenger trains. Numbers 11–27 represent all universal trains A1-A10 and B1-B7 (Table 1). As shown, HSLM-B4 and HSLM-A2 are the shortest trains, and the longest ones are represented by number 12 and number 24 with 5 and 398.5 meters long, respectively. Given the different geometries of real high-speed trains and Eurocode HSLM, a total of 27 distinct train geometries are gathered to pursue a comprehensive and detailed study on the behavior of bridges under high-speed trains. The multi-axle-moving-force models are used to perform dynamic analyses.

Research studies have shown that increasing details of vehicle modeling is only impressive in the resolution of calculating vehicle responses and has no remarkable effect on bridge responses [3]. Therefore, it is reasonable to use fewer details to simulate the moving vehicular loads since the aim is to investigate the behavior of bridges in this study. Therefore, concerning the purpose of the present study, investigating the bridges' responses, the trains axles were crossed over the bridges as concentrated moving forces at certain distances [3]. The intended speeds of the moving loads in the study are limited to 75 and 400 km/h, respectively 20.8 and 111.1 m/s.

Vehicle type and characteristics are vital parameters in the realistic prediction of bridge load-carrying capacity and its dynamic response. While many different models (some very complicated) have been provided before, it is generally agreed that, in the face of complex random loading, none can meet all conceivable probabilities. Using Eurocode HSLM, the dynamic behavior of masonry arch bridges may not be properly assessed. So, an effort has been made to analyze the behavior of these bridges under real high-speed trains to tackle the results with more reliance.

3 DAF description

The DAF is an applicable term to design and analyze the dynamic behavior of bridges. As the response of bridges caused by static vehicular loads increases, the dynamic behavior of structures is considered.

The term DAF increases static loads by applying them then takes the effects of trains' dynamic loads into consideration. This method has focused on different types of bridges, including highway and railway bridges of guidelines.

The DAF is calculated by employing the values of the dynamic and static responses (deflections, bending moments, or shear forces) of bridges [1]. Earlier studies indicated that the DAF obtained by taking the deflection in the midspan achieved equivalence to the values based on strain [33, 34]. According to the analyses performed in the present study and the outputs obtained, in the current study, the dynamic load effects on the bridge are measured in terms of the maximum dynamic and static deflections. The DAF is described using the allowable dynamic load allowance (DLA) based on the maximum values of dynamic and static responses in the midspan of the bridges and given by Eq. (1) [7]:

$$DLA = \frac{D_{dyn} - D_{sta}}{D_{sta}} \quad \text{or} \quad DLA + 1 = \frac{D_{dyn}}{D_{sta}} = DAF, \quad (1)$$

where D_{dyn} and D_{sta} denote, respectively the maximum dynamic and static deflections, in mm, of the bridges calculated in the midspan.

4 Guidelines suggestions for railway bridges

This section describes guideline considerations for computing DAF of railway bridges in regular and high-speed conditions.

4.1 Regular speed vehicles

The DAF equations of different railway bridge standards are described based on diverse main variables [27, 35, 36]. Train speed, bridge type, span length, and the first vibration frequency are some of the mentioned parameters. As an impressive parameter on the dynamic response of bridges, span length (L) has been distinguished in most current bridge design codes. American railway engineering and maintenance of way (AREMA) has defined the DAF as follows [36]:

$$DAF = \begin{cases} (40 - \frac{3L^2}{148.6})/100 & L \leq 24 \\ (16 + \frac{182.9}{L-9.1})/100 & L > 24 \end{cases}. \quad (2)$$

Eurocode suggests following relationships for DAF to be calculated in simplified method [27]:

$$DAF = \begin{cases} \frac{2.16}{\sqrt{L_\phi - 0.2}} + 0.73 & \text{standard maintenance} \\ \frac{1.44}{\sqrt{L_\phi - 0.2}} + 0.82 & \text{carefully maintained tracks} \end{cases}, \quad (3)$$

where L_ϕ is in meters and the determinant length is equivalent to twice the clear opening for masonry arch bridges.

Iranian standard loads for bridges utilizes two DAF equations for rail application depending on the track maintenance condition as well as the simplified method of Eurocode (Eq. (3)). Where L_ϕ is in meters and the determinant length is equivalent to half span.

Train speed and first vibration frequency are also main parameters on the dynamic response identified in some other codes. Eurocode detailed method (Eq. (4) to Eq. (8)) and Ontario railway regulations (ORE) (Eq. (9)) fall into this category based on DAFs below [27]:

$$DAF = \begin{cases} 1 + \phi' + \phi'' & \text{standard maintenance} \\ 1 + \phi' + 0.5\phi'' & \text{carefully maintained tracks} \end{cases}, \quad (4)$$

where ϕ' and ϕ'' are computed by Eq. (5).

$$DAF = \begin{cases} \phi' = \frac{K}{1 - K + K^4} & K < 0.76 \\ \phi' = 1.325 & K \geq 0.76 \end{cases}, \quad (5)$$

where

$$K = \frac{v}{2L_\phi n_0}, \quad (6)$$

and

$$\phi'' = \frac{\alpha}{100} \left[56e^{-\left(\frac{L_\phi}{10}\right)^2} + 50\left(\frac{L_\phi n_0}{80} - 1\right)e^{-\left(\frac{L_\phi}{20}\right)^2} \right], \quad (7)$$

with

$$\begin{cases} \alpha = \frac{v}{22} & v \leq 22 \text{ (m/s)} \\ \alpha = 1 & v > 22 \text{ (m/s)} \end{cases}. \quad (8)$$

In the aforementioned equations, v denotes train speed in m/s, n_0 is the first bending frequency of the structure, L_ϕ is the determinant length in m, and α is train speed coefficient.

ϕ' maintains the rate of loading due to the traffic load speed. It also covers the effects of the passage of successive loads which may excite the structure and cause resonance. ϕ'' covers the effects of variations in wheel loads resulting from track or vehicle imperfections.

ORE has the same perspective on main parameters on extracted dynamic response as Eurocode does (Eq. (9), Eq. (10)) [35].

$$DAF = \frac{0.65K}{1 - K + K^2}, \quad (9)$$

where

$$K = \frac{v}{2Lf}, \quad (10)$$

where v denotes vehicle's speed in m/s, f is the first bending frequency of the structure, and L is span length in m.

4.2 High-speed vehicles

DAF equations used on old railway bridges or highway bridges cannot be used for high-speed railway bridges. Railway regulations of various countries, including Eurocode, consist of specific rules for high speeds on railways and some of which have been represented in Eq. (4) to Eq. (8). The dynamic responses of bridges including stress, deflection, and acceleration caused by high-speed moving loads are greater than low-speed ones [6]. So, the dynamic performance of bridges under high-speed dynamic loads may become more complicated. Furthermore, modern high-speed trains pose serious challenges to bridge design and maintenance in terms of the dynamic load they have to be able to bear. Therefore, there is a great demand for keeping structures subjected to moving loads reliable by considering the effects caused by them.

Hence, more expanded analyses and experimental studies should be performed about it. Moreover, the dynamic response of masonry arch bridges to high-speed trains traveling on these structures can be scientifically stepped into the spotlight through this study. Accordingly, we try to clarify the correlation between the bridges' dynamic behavior and impressive parameters, comprising bridge length, number of spans, and train length, by calculating the DAF.

There are not several standards giving serious consideration to the debate about calculating the DAF of bridges under high-speed trains. According to Eurocode, For structures imposed by dynamic loads at speeds over 200 km/h, the aforementioned dynamic amplification factor may be insufficient and may need to be determined by a dynamic analysis [27]. So, the dynamic analysis shall be undertaken using characteristic values of the loading from HSLM and the specific Real Trains [27]. However, Eq. (4) to Eq. (8), regarding the Eurocode detailed method, as mentioned before, state how DAF to be calculated at speeds higher than 80 km/h [27]. Iranian regulations for design and inspection of the high-speed railway network,

propose DAFs maintaining track condition and vehicle's speed. The DAF is equivalent to 1.5 for speeds below 200 km/h and 1.75 for speeds over 200 km/h.

Nevertheless, accurate estimations of DAFs of bridges under high-speed trains, to some extent, have not gone under the heading of the code provisions.

4.3 Guidelines for masonry arch bridges

A common practice of analyzing railway bridges exerted by dynamic effects of a moving train is to apply the DAF defined by design codes. It is shown that the dynamic responses of bridges are expressed by DAF, and the vertical acceleration parameter of the vehicle is used to evaluate passenger comfort. In recent years, extensive studies have been carried out to validate the regulatory equations and compare them with the results of field and numerical results. Despite all the inherent advantages of masonry arch bridges, they create challenging problems for engineers in assessing their DAF for evaluation of the dynamic behavior. Thus, while masonry arch bridges have formed a large number of existing railway bridges, the design codes are rather focused on the rest of the bridge stock of the railway network. Most research studies have concentrated on developing the dynamic behavior assessment of RC and steel railway bridges.

There are a few experimental and analytical research papers performed on investigating the correlation between DAF and train-masonry arch bridges characteristics [3, 16]. However, according to the international union of railways (UIC), the most reliable relations regarding DAF have been expressed for masonry arch bridges in UIC Code [37]. Nevertheless, this issue needs to be further addressed.

5 Numerical modeling

Owing to the deterioration of masonry and the complexity of details, numerical simulation is necessary to evaluate the dynamic behavior of masonry arch bridges. The discrete element method (DEM) and finite element approach (FEM) have been widely used for numerical simulation of the masonry arch bridges in both the macro-modeling and the micro-modeling methods [38–42].

5.1 Finite element analysis

In the present study, the finite element method and macro modeling approach are used as efficient methods to prepare a numerical model. Different components of the structures, including arches, abutment, spandrel, and wing walls, are simulated in accordance with the real condition of the bridges and concerning details. Also, according to the in-plane behavior of masonry arch bridges under vertical load, plane strain analysis is used in the simulation process. The investigated structures are two old bridges (2L20 and 5L06 bridges) depicted in Fig. 2, and their geometric characteristics are presented in Table 2.

The modeling procedure consisted of two parts related to the bridges simulated through the finite element method and the moving load method used to investigate the dynamic effect of the moving trains on the structures. The results of several research papers show that increasing the detail of vehicle modeling is only effective in boosting the accuracy of calculating vehicle responses and has no significant effect on bridge responses. One of these cases is a recent study on the dynamic behavior of masonry arched

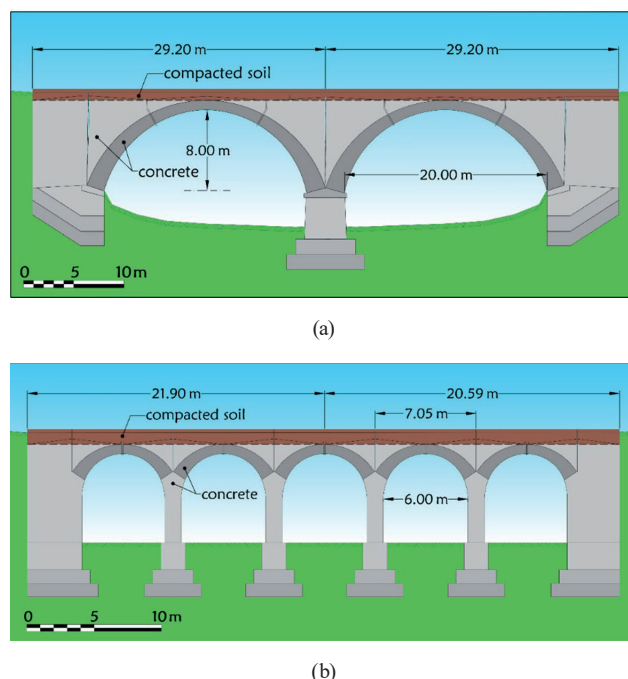


Fig. 2 Geometric characteristics of bridges: (a) 2L20 and (b) 5L06 (units are in meter)

Table 2 Geometric characteristic of the bridges

Bridge	No of spans	Span's length (m)	Shape of arch	Thickness of crown (m)	Thickness of arch ends (m)	Arch width (m)	Bridge height (m)	Thickness of spandrel walls (m)
Km-23	2	20	Segment of circle	1	1.9	3.9	12	1
Km-24	5	6	Half circle	0.7	1.1	3.9	8	1

bridges [3]. Therefore, since the present study intends to investigate bridges' responses, it is reasonable to use fewer details to simulate vehicles. Not only does this approach increase the accuracy of the results, but it also reduces computational costs. Accordingly, in the present study, a moving load model is used to simulate the train load crossing the bridges instead of the moving mass model.

Finally, due to the principal two-dimensional behavior displayed by masonry arch bridges under vertical loads and according to Fig. 3, the finite element models have been shown. In the present numerical model, four-node and high-order eight-node elements are utilized. In total, a finite element model of 7505 elements and 16129 nodes (equivalent to 32258 degrees of freedom) is formed for the 2L20 bridge, and 8040 elements and 16674 nodes (equivalent to 33348 degrees of freedom) is formed for the 5L06 bridge.

The bridges were both built more than 80 years ago, and all parts, including arches, wing walls, spandrels, piers, and foundations are constructed using unreinforced concrete. By taking cylindrical cores from different parts of the bridges, the quality of concrete is determined, and the mechanical properties of the plain concrete are extracted as a result of the test and reported by Marefat et al. [43, 44]. The present study focuses on arches with small fill material heights, because test data show that there is a considerable reduction in the dynamic amplification factor for arch bridges with depths of cover greater than 1. During the bridge simulation process, the materials were assumed to behave non-linearly, and the Drucker-Prager yielding criterion has been implemented to predict possible failures. For this purpose, the mechanical properties of the

materials are considered according to Table 3. It is noteworthy that the equation has been used to calculate the tensile strength of concrete in accordance with their compressive strength, and all their nonlinear characteristics have been obtained based on this assumption.

5.2 Verification

In order to validate the presented models, static analysis, modal analysis, and dynamic analysis have been conducted, and the results have been compared with the field test outputs. The static experiment was carried out using the weights of 40 kN on the right span of the 2L20 bridge and the midspan of the 5L06 bridge. The static test continued until the load of 7280 kN was applied on the 2L20 bridge and 5000 kN on the 5L06 bridge. The vertical displacement of the bridges was recorded at the crowns under the effect of these loads [44, 45]. Fig. 4 displays the results of nonlinear static analysis of the numerical model compared with the field test results reported by Marefat et al. [43, 44]. In the second step of validation of the proposed models, using modal analysis, the three fundamental frequencies of the numerical model are calculated and compared with the experimental results in Table 4.

According to Fig. 5, the error between non-linear static analysis and the experimental results of the 2L20 and 5L06 bridges equals 8 and 1.5 percent, respectively. Table 4 provides a summarized comparison between the gained frequencies of the first three modes from the natural frequencies of the bridges calculated based on experimental test and finite element method. The average error between the modal analysis of the numerical model and the field test results of 2L20 and 5L06 is equal to 7.4 and 5.9 percent, respectively.

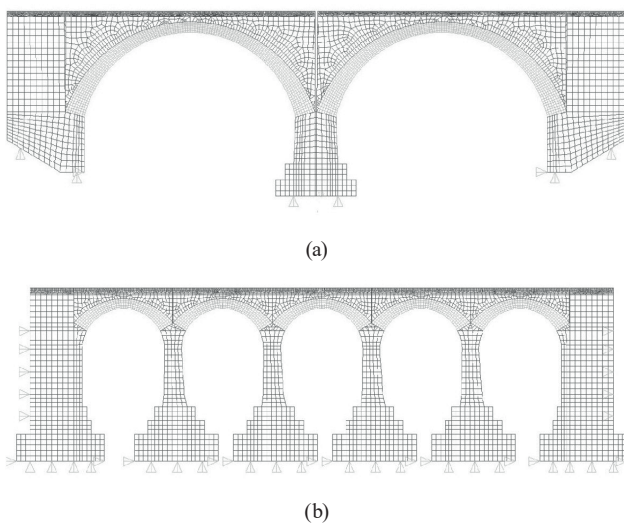
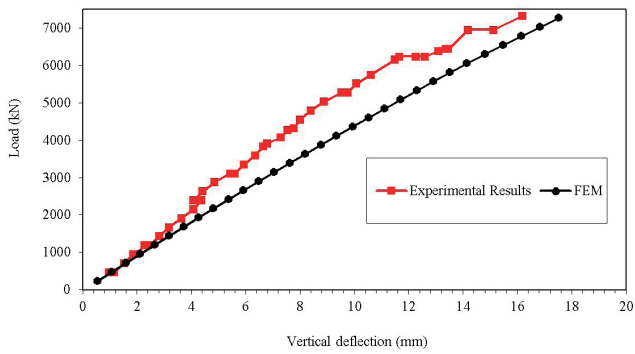


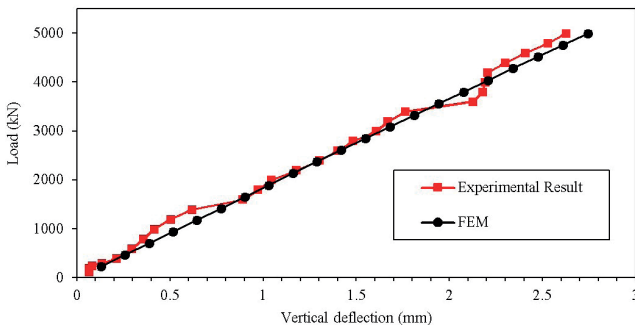
Fig. 3 Finite element model of the bridges: (a) 2L20, (b) 5L06

Table 3 Final properties of materials after calibration

Item	Density (kg/m ³)	Modulus of elasticity (GPa)	Poisson ratio	Cohesion (KPa)	Friction angle (degree)	Dilatancy angle (degree)
Bridge	2L20	2L20	2L20	2L20	2L20	2L20
	5L06	5L06	5L06	5L06	5L06	5L06
Fill-material	2300	8.50	0.25	1750	36.5	36.5
	2217	10.90	0.29	1915	34.5	34.5
Arch	2280	17.00	0.21	3370	47.4	47.4
	2290	24.90	0.17	6591	53.0	53.0
Pier & wing wall	2350	37.30	0.19	5100	51.2	51.2
	2250	36.50	0.18	5617	49.8	49.8
Ballast	2300	8.50	0.25	----	----	----
	2000	7.00	0.33	----	----	----



(a)



(b)

Fig. 4 Static analysis in comparison with experimental results at crown: (a) right span of 2L20 bridge and (b) midspan of 5L06 bridge

Table 4 The natural frequencies of the bridges at first three modes in the Locomotive test and FE models in Hz

Bridge name	Case	First mode	Second mode	Third mode
2L20	Experimental	4.48	7.91	10.83
	FEM	4.11	8.84	10.56
	Error (%)	9.0	10.6	2.6
5L06	Experimental	14.6	21.5	26.4
	FEM	15.42	22.36	28.38
	Error (%)	5.6	4.0	8.3

Finally, in the last calibration level, using non-linear dynamic analysis, the six-axes locomotive, shown in Fig. 5, was passed on the numerical models of 2L20 and 5L06 at a speed of 60 km/h and 80 km/h. The dynamic analysis is conducted using time-history method along with Rayleigh’s damping model implemented to consider the damping ratio. Finally, the time-history dynamic analyses were carried out by implementing the Newmark-Beta technique, and its results are presented in Fig. 6. It is valuable to say that the maximum response is the fundamental parameter in comparison between experimental test and numerical model results, so according to the results obtained from Fig. 6, the error between the maximum numerical model response and the diesel moving load tests of the 2L20 and 5L06 are equal to 1 and 1.4 percent, respectively. It should

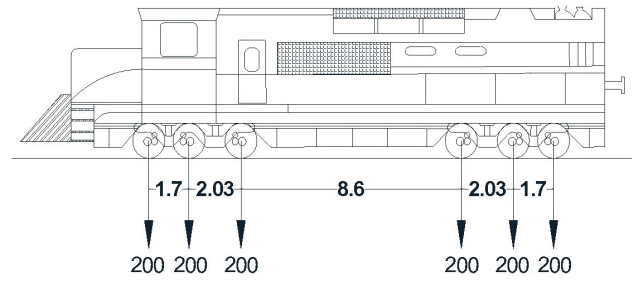
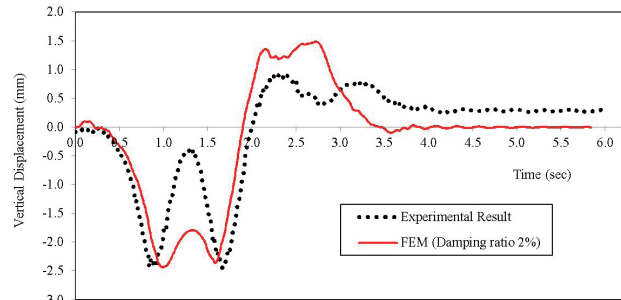
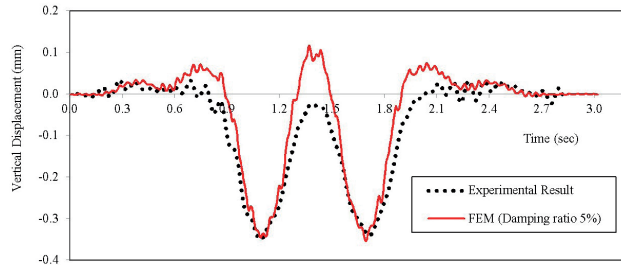


Fig. 5 Six-axes locomotive moving load used in dynamic test



(a)



(b)

Fig. 6 Dynamic response of the bridges at the crown: (a) 2L20, for a speed of 60 km/h in the left span and (b) 5L06, for a speed of 80 km/h in the midspan

be noted that several references have reported that the damping ratio of masonry arch bridges is between 1% and 10 %, in which the value decreases with increasing the span length [46]. Therefore, for the 2L20 bridge, a damping ratio of 2% and for the 5L06 bridge, a damping ratio of 5% is assumed so that the maximum displacement values are the same in the numerical and experimental outcomes. According to the results obtained from the numerical model, it can be inferred that the numerical model has been successfully validated and it can be concluded that the presented finite element model has the ability to display other dynamic characteristics of the structure.

5.3 Sensitivity analysis

Five key parameters like train length (L_t), bogies intervals (I_b), axles intervals (I_a), bridge length (L_b), and span length (L_s) were defined to evaluate the DAFs. A sensitivity analysis was conducted first to investigate the effect of

these parameters on the dynamic response of the prototype bridges. Then, four critical concepts included train length to bridge length ratio (L_t/L_b), train length to span length ratio (L_t/L_s), bogies intervals to span length ratio (I_b/L_s), and axles intervals to span ratio (I_a/L_s) were extracted. The sensitivity study revealed that the change in the parameters has a significant effect on the DAFs. In the first step, a comprehensive sensitivity analysis is designed and performed to evaluate the effects of the aforementioned parameters covering different classifications of realistic masonry arch bridges in terms of bridge span length which exist nowadays in conventional railway lines. To this end, a couple of masonry arch bridges, with span lengths ranging from 6 to 20 meters, different total length of bridges, and a different number of spans is opted for this study.

Due to the increasing use of high-speed trains, studies concerning the dynamic behavior of high-speed railway bridges have developed recently. Accordingly, although, numerous studies have been conducted to investigate the dynamic behavior of railway bridges under the effect of vehicles traveling at high speeds, no consensus on this subject has been reached yet and many previous studies have been led to different findings. In the second step, the outputs of the presented equations in the regulations can

be compared with the values obtained from the sensitivity analyses. Besides, the possibility of using the DAF method for masonry arch bridges can be studied as an alternative method. To do so, the correlation between DAF values and the aforementioned effective parameters on the dynamic behavior of the bridges is depicted in Fig. 7. As it is shown, Fig. 7 displays the effect of the different parameters on DAFs at any speed value due to both real trains and HSLM trains distinctively. Since the consideration of higher speeds does not seem essential, the considered speeds of the moving loads in the present study are restricted by the range of 75 and 400 km/h, corresponding to 20.8 and 111.1 m/s. So, Fig. 7 contains 4 scatter charts in which 378 values of DAF are represented.

Fig. 8 depicts the maximum DAF values of the bridges exerted by real trains and HSLM at every speed. So, it consists of 4 charts with 54 symbols to show how the considered parameters affect the peak values changes. Plus, the peak values of the DAFs are sorted by the trains' categories in Fig. 8.

6 Discussion

The following results can be concluded based on the DAF values of the numerical models displayed in Figs. 7 and 8:

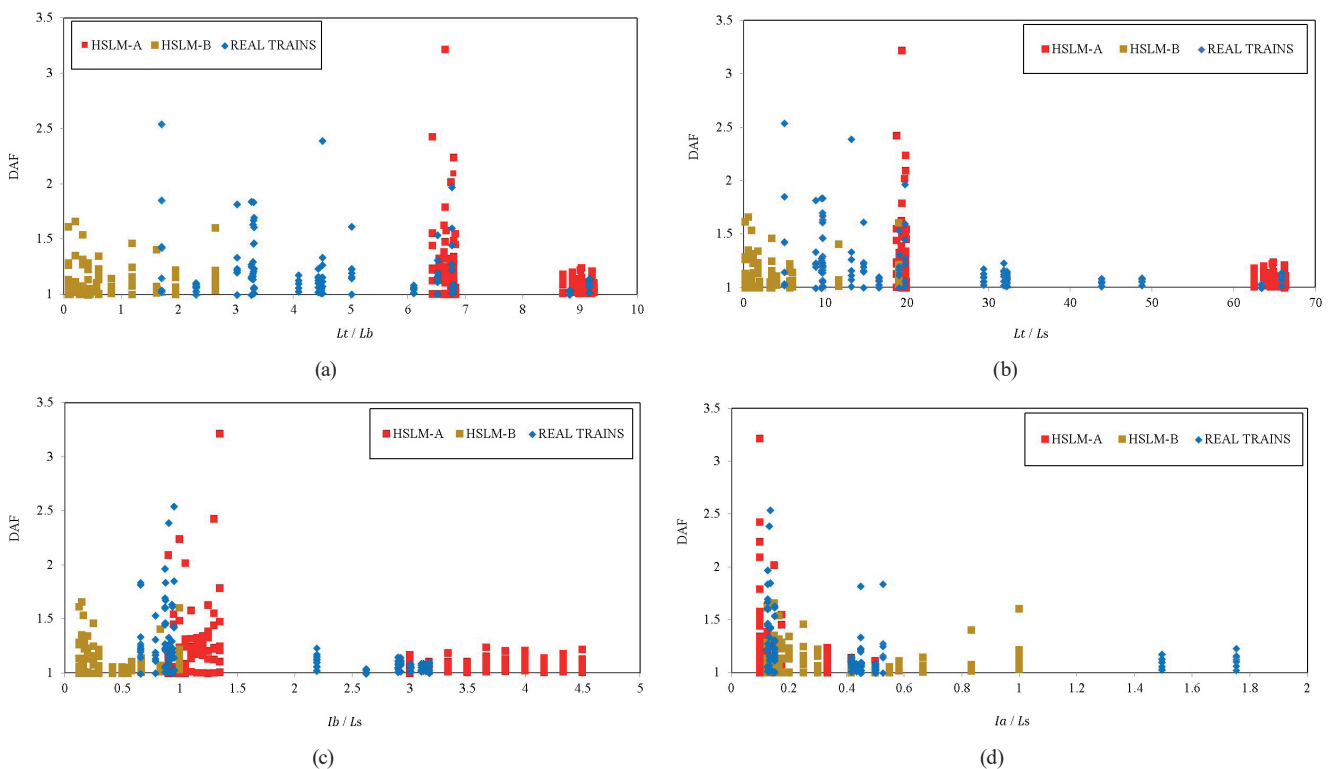


Fig. 7 The DAF values of the bridges at various speeds according to: (a) Train length to bridge length ratio, (b) Train length to span length ratio, (c) Bogies interval to span length ratio, (d) Axles interval to span length ratio

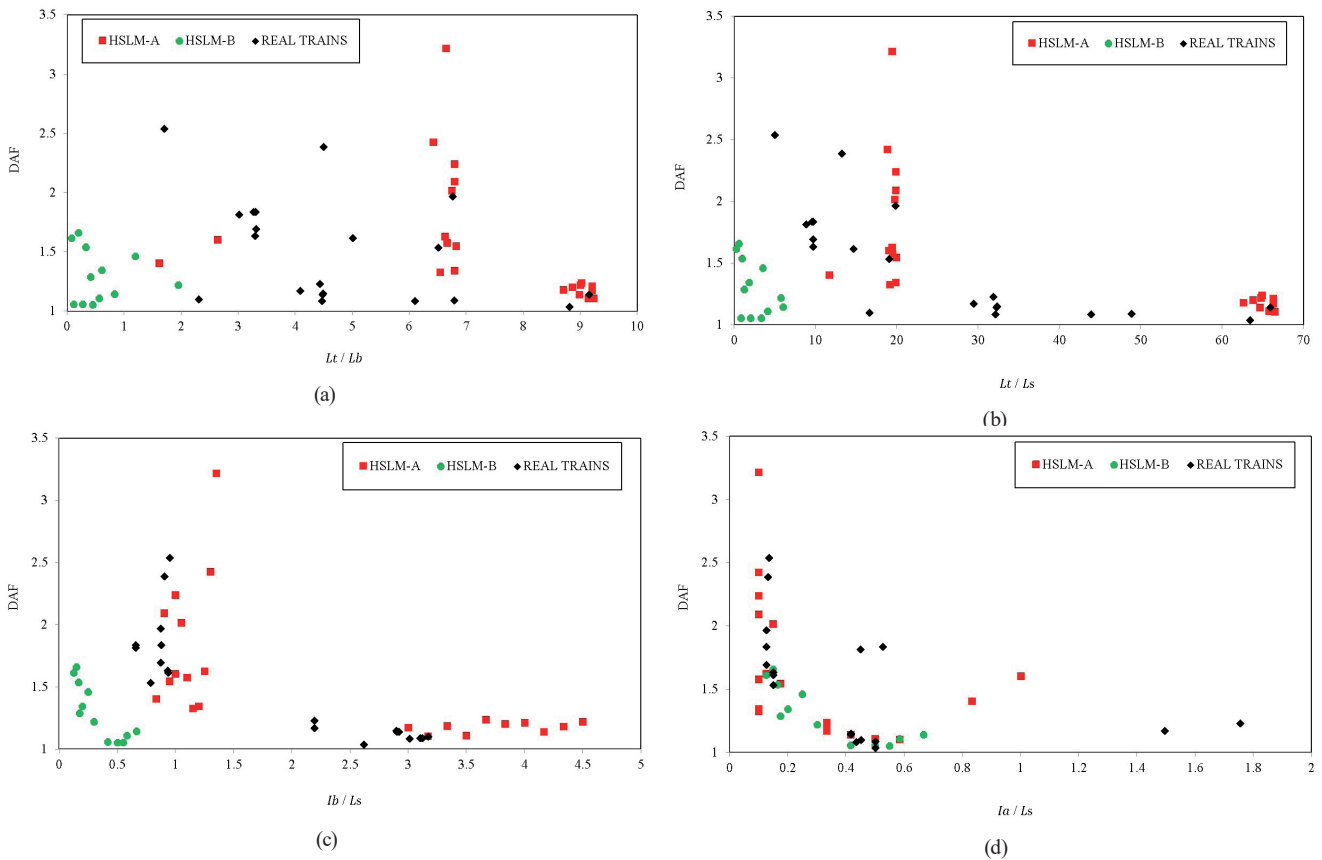


Fig. 8 The maximum DAF values of the bridges at every speed according to: (a) Train length to bridge length ratio, (b) Train length to span length ratio, (c) Bogies interval to span length ratio, (d) Axles interval to span length ratio

- The minimum and the maximum DAFs are equal to 1 and 3.2, respectively. The maximum DAF value of the bridges is obtained under A10 of the HSLM category, whereas the minimum DAF is calculated under the number of real and Eurocode high-speed trains (See Fig. 7). The peak DAFs of the bridges exposed by the moving real high-speed trains are between 1 and 2.5. As HSLM, type A is larger than type B, the HSLM-A family has a bigger quantity in train length to bridge length ratio and the HSLM-A family reaches the higher DAFs as well. The most critical condition takes place when train length to bridge length ratio is equal to 6.6. As the parameter increases from this value, fewer numbers of DAF are displayed. The minimum value of train length to bridge length ratio, in the HSLM category, is 0.1 related to B4, and the maximum value is 9.2 which is related to A7. These values in real trains are 1.7 and 9.1 produced by Renfe S104 and ICE, respectively. As it is evident, train length to bridge length ratio is restricted by the range of 1.7 to 9.16 for real trains and 0.1 to 9.2 for HSLM. It shows that Eurocode predicts a desirable range of DAF and

train length to bridge length ratio parameter which contains any type of real trains even though real trains do not represent a specific trend (See Fig. 7).

- The minimum value of train length to span length ratio, in the HSLM category, equals 0.25 related to B4, and the maximum value is 66.2 which is related to A7. These parameters in real trains are 5 and 65.8 related to Renfe S104 and ICE, respectively. Despite the increase in train length to span length ratio, there is no specific visible pattern in DAF changes of real trains. HSLM-A family has larger amounts of train length to span length ratio than HSLM-B due to the larger train models and type A also has a bigger quantity of DAF. It is worth mentioning that Eurocode provides acceptable values comparing real trains in terms of train length to span length ratio parameter. According to the peak values of DAF, it is deduced that when train length to span length ratio is equal to 19.4, the maximum DAF is produced. By passing the maximum DAF and with increasing train length to span length ratio the DAF values decrease considerably (See Fig. 7).

- The minimum value of bogies interval to span length ratio, in the HSLM category, is equal to 0.12 related to B4, and the maximum value is 4.5 related to A10. These parameters in real trains equals 0.7 and 3.2 related to Renfe S130 and Renfe S104, respectively. It is interpretable that Eurocode overestimates this parameter according to the ratios obtained from real trains in comparison with HSLM. When bogies interval to span length ratio equals 1.3, DAF reaches 3.2 as its maximum value. From this point on, the DAFs decrease with increasing bogies interval to span length ratio (See Fig. 7).
 - Despite the aforementioned parameters, axles interval to span length ratio represents the different pattern. Bogies interval, however, has a directed correlation with bridge length, although axles interval and bridge length are inversely correlated (See Fig. 7). The most critical condition happens when axles length to span length ratio is equal to 0.1 and the DAFs decrease with increasing axles interval to span length ratio. With increasing axles interval to span length ratio, the DAF values tend to 1.
 - Based on the obtained responses as DAF values in the present study, the median of these data is equal to 1.089, their average equals 1.168, and the standard deviation is equal to 0.246. The sum of the mean and the standard deviation values of these data shows the number of 1.414 and 90% of these indicated dynamic amplification factors are less than 1.414.
 - Due to the study reports in numerous cases on the dynamic behavior of railway bridges, 99.7% of all DAF values vary from 1 to 2.6. With respect to the obtained responses as DAF values in the study, the maximum DAF value of the bridges subjected to Renfe S100 equals 1.64. This parameter shows different values under real high-speed trains equal to 1.84, 1.7, 2.54, 1.82, 2.4, 1.54, 1.84, 1.62, and 1.97 produced by Renfe S102, Renfe S103, Renfe S104, Renfe S130, China Star, KHST, SKS, TGV, and ICE, respectively (See Fig. 8). According to obtained DAF values, KHST has the lowest peak DAF, and Renfe S104 has the highest peak DAF among the real high-speed trains.
 - More than 50% of the obtained DAFs are between 1 and 1.1, and less than 8% of the DAF values are more than 1.5. The frequency of DAF was found to reduce with the increase of the values of this parameter.
- Accordingly, the frequency of DAF values more than 2.1 equals 5. KHST is chosen as a train with the best performance because it produces the lowest peak DAF value when the train travelled on the 2L20 at 300 km/h and Renfe S104 as a train with the worst performance in this case because of the highest DAF occurred when it travelled on the 2L20 at 400 km/h.
- Based on the calculated DAFs in the present study, and according to Fig. 7, there are 378 indicated values of DAF in each scatter chart, and 92% of these values have dynamic amplification factors of less than 1.5. The median of these data is equal to 1.089, their average equals 1.168, and the standard deviation is equal to 0.246. The sum of the mean and the standard deviation values of these data shows the number of 1.414, and 90% of these indicated dynamic amplification factors are less than 1.414
 - There is no apparent relation between the speed and DAF values. So, DAF does not represent a constant direct or inverse correlation with the speed of moving vehicles.
 - The DAFs of the 2L20 have higher values in comparison with the corresponding DAF values of the 5L06 at the same speeds. Accordingly, it is understood that the DAFs are directly correlated with the bridge length.
 - As it is depicted in Fig. 8, bogies interval to span ratio and axles interval to span ratio against DAF, display specific smooth trend while two other parameters do not tend to show any particular trend in resulting charts.
 - According to the maximum DAF values charts shown in Fig. 8, it is deduced that bogies interval, axles interval, and span length play a crucial role in calculating DAFs while train length and bridge length are not such significant parameters as Eurocode considers axles interval as one of the most important parameters in terms of the dynamic behavior of railway bridges exposed to the movement of trains.
 - According to the considerations, the obtained DAF values of HSLM (type A) have a bigger quantity than real trains, thus representing the proper intended safety factor of Eurocode.
 - Fig. 9 shows the trend of the maximum DAF values via axles interval to span ratio. It is indicated that the approximated function matches 44 out of 50 data entries.

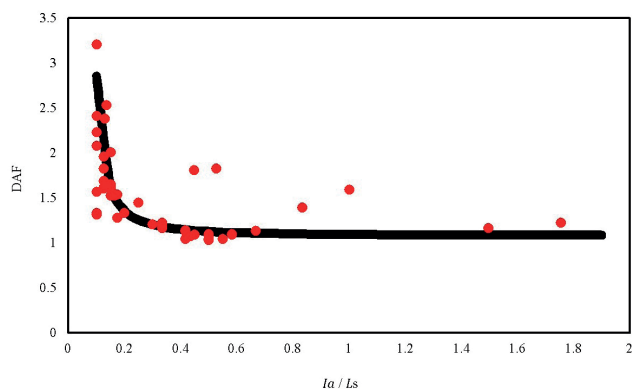


Fig. 9 The trend of peak DAF values of the bridges via axles interval to span length ratio

7 Conclusions

There are about 3300 masonry arch bridges out of 30000 railway bridges in Iran. The existing masonry arch bridges cannot be replaced because of time, field, and economic constraints. That is why dynamic analyses have to be performed to determine the safety and reliability of these bridges. On the other hand, because of the increasing demand for reducing traffic time, higher speeds on railway networks lead us to the maximum use of the existing structures. So, it is necessary to evaluate the dynamic behavior of these bridges under the effect of high-speed trains. Numerical models can be very expensive in relation to practical use in engineering. Hence, in order to be able to perform calculations in a satisfactory amount of time, the simplicity of the model and the size of the model are

important considerations. As it is discussed, bogies interval, axles interval, and span length are recognized as the most important parameters in the DAFs changes. Almost all of the determined DAFs vary within 1 and 2.6, however, a majority of these values are less than 1.1 and few cases exceed a value of 1.7. Based on the indicated data in this research, the median of DAFs is equal to 1.089, the average equals 1.168, and the standard deviation is 0.246. The sum of the mean and the standard deviation values of these data shows the number of 1.414, and 90% of these DAF values are less than 1.414. Due to the limit, KHST has the best performance among all the investigated trains and Renfe S104 displays the worst performance.

It is necessary to mention that, there is no high-speed train in Iran right now. So, these conclusions based on mentioned responses can be appropriate but, it seems by implementation some consideration the behavior of masonry arch bridges under high-speed trains in railway networks may be acceptable, and it is recommended to use the Korean high-speed train in Iran railway network. Since the 2L20 and 5L06 bridges are settled in the medium-sized bridges category, as a conclusion, KHST can be deduced as the best high-speed train in terms of the dynamic amplification factor to impose on these bridges. Also, it can be concluded that the maximum DAF values via axles interval to span ratio is the most important parameter for the dynamic assessment of railway masonry arch bridges under high-speed trains.

References

- [1] Majka, M., Hartnett, M. "Effects of speed, load and damping on the dynamic response of railway bridges and vehicles", *Computers & Structures*, 86(6), pp. 556–572, 2008.
<https://doi.org/10.1016/j.compstruc.2007.05.002>
- [2] Delgado, R. E., Calcada, R., Goicolea, J. M., Gabaldon, F. (eds.) "Dynamics of High-Speed Railway Bridges", 1st ed., CRC Press, London, UK, 2008.
- [3] Forgács, T., Sarhosis, V., Ádány, S. "Shakedown and dynamic behaviour of masonry arch railway bridges", *Engineering Structures*, 228, 111474, 2020.
<https://doi.org/10.1016/j.engstruct.2020.111474>
- [4] Galvín, P., Romero, A., Moliner, E., De Roeck, G., Martínez-Rodrigo, M. D. "On the dynamic characterisation of railway bridges through experimental testing", *Engineering Structures*, 226, 111261, 2021.
<https://doi.org/10.1016/j.engstruct.2020.111261>
- [5] H. Gou, H., Xie, R., Liu, C., Bao, Y., Pu, Q. "Analytical study on high-speed railway track deformation under long-term bridge deformations and interlayer degradation", *Structures*, 29, pp. 1005–1015, 2021.
<https://doi.org/10.1016/j.istruc.2020.10.079>
- [6] Yazdani, M., Azimi, P. "Assessment of railway plain concrete arch bridges subjected to high-speed trains", *Structures*, 27, pp. 174–193, 2020.
<https://doi.org/10.1016/j.istruc.2020.05.042>
- [7] H. Moghimi, H., Ronagh, H. R. "Impact factors for a composite steel bridge using non-linear dynamic simulation", *International Journal of Impact Engineering*, 35(11), pp. 1228–1243, 2008.
<https://doi.org/10.1016/j.ijimpeng.2007.07.003>
- [8] Deng, L., He, W., Shao, Y. "Dynamic Impact Factors for Shear and Bending Moment of Simply Supported and Continuous Concrete Girder Bridges", *Journal of Bridge Engineering*, 20(11), 04015005, 2015.
[https://doi.org/10.1061/\(ASCE\)BE.1943-5592.0000744](https://doi.org/10.1061/(ASCE)BE.1943-5592.0000744)
- [9] Deng, L., Wang, F. "Impact Factors of Simply Supported Prestressed Concrete Girder Bridges due to Vehicle Braking", *Journal of Bridge Engineering*, 20(11), 06015002, 2015.
[https://doi.org/10.1061/\(ASCE\)BE.1943-5592.0000764](https://doi.org/10.1061/(ASCE)BE.1943-5592.0000764)
- [10] Huang, D. "Vehicle-Induced Vibration of Steel Deck Arch Bridges and Analytical Methodology", *Journal of Bridge Engineering*, 17(2), pp. 241–248, 2012.
[https://doi.org/10.1061/\(ASCE\)BE.1943-5592.0000243](https://doi.org/10.1061/(ASCE)BE.1943-5592.0000243)

- [11] M. Samaan, M., Kennedy, J. B., Sennah, K. "Impact Factors for Curved Continuous Composite Multiple-Box Girder Bridges", *Journal of Bridge Engineering*, 12(1), pp. 80–88, 2007.
[https://doi.org/10.1061/\(ASCE\)1084-0702\(2007\)12:1\(80\)](https://doi.org/10.1061/(ASCE)1084-0702(2007)12:1(80))
- [12] Wang, W., Deng, L. "Impact Factors for Fatigue Design of Steel I-Girder Bridges Considering the Deterioration of Road Surface Condition", *Journal of Bridge Engineering*, 21(5), 04016011, 2016.
[https://doi.org/10.1061/\(ASCE\)BE.1943-5592.0000885](https://doi.org/10.1061/(ASCE)BE.1943-5592.0000885)
- [13] Deng, L., Yu, Y., Zou, Q., Cai, C. S. "State-of-the-Art Review of Dynamic Impact Factors of Highway Bridges", *Journal of Bridge Engineering*, 20(5), 04014080, 2015.
[https://doi.org/10.1061/\(ASCE\)BE.1943-5592.0000672](https://doi.org/10.1061/(ASCE)BE.1943-5592.0000672)
- [14] L. Ma, L., Zhang, W., Cai, C. S., Li, S. "The dynamic amplification factors for continuous beam bridges along high-speed railways", *Advances in Structural Engineering*, 24(11), pp. 2542–2554, 2021.
<https://doi.org/10.1177/13694332211003288>
- [15] Lee, H.-H., Jeon, J.-C., Kyung, K.-S. "Determination of a reasonable impact factor for fatigue investigation of simple steel plate girder railway bridges", *Engineering Structures*, 36, pp. 316–324, 2012.
<https://doi.org/https://doi.org/10.1016/j.engstruct.2011.12.021>
- [16] Ataei, S., Miri, A. "Investigating dynamic amplification factor of railway masonry arch bridges through dynamic load tests", *Construction and Building Materials*, 183, pp. 693–705, 2018.
<https://doi.org/10.1016/j.conbuildmat.2018.06.151>
- [17] Au, F. T. K., Wang, J. J., Cheung, Y. K. "Impact study of cable-stayed railway bridges with random rail irregularities", *Engineering Structures*, 24(5), pp. 529–541, 2002.
[https://doi.org/10.1016/S0141-0296\(01\)00119-5](https://doi.org/10.1016/S0141-0296(01)00119-5)
- [18] Gou, H., Zhou, W., Chen, G., Bao, Y., Pu, Q. "In-situ test and dynamic response of a double-deck tied-arch bridge", *Steel and Composite Structures*, 27(2), pp. 161–175, 2018.
<https://doi.org/10.12989/SCS.2018.27.2.161>
- [19] Cheng, Y. S., Au, F. T. K., Cheung, Y. K. "Vibration of railway bridges under a moving train by using bridge-track-vehicle element", *Engineering Structures*, 23(12), pp. 1597–1606, 2001.
[https://doi.org/10.1016/S0141-0296\(01\)00058-X](https://doi.org/10.1016/S0141-0296(01)00058-X)
- [20] Hamidi, S. A., Danshjo, F. "Determination of impact factor for steel railway bridges considering simultaneous effects of vehicle speed and axle distance to span length ratio", *Engineering Structures*, 32(5), pp. 1369–1376, 2010.
<https://doi.org/10.1016/j.engstruct.2010.01.015>
- [21] Xia, H., De Roeck, G., Zhang, N., Maeck, J. "Experimental analysis of a high-speed railway bridge under Thalys trains", *Journal of Sound and Vibration*, 268(1), pp. 103–113, 2003.
[https://doi.org/10.1016/S0022-460X\(03\)00202-5](https://doi.org/10.1016/S0022-460X(03)00202-5)
- [22] Kwark, J. W., Choi, E. S., Kim, Y. J., Kim, B. S., Kim, S. I. "Dynamic behavior of two-span continuous concrete bridges under moving high-speed train", *Computers & Structures*, 82(4), pp. 463–474, 2004.
[https://doi.org/10.1016/S0045-7949\(03\)00054-3](https://doi.org/10.1016/S0045-7949(03)00054-3)
- [23] Yau, J.-D., Yang, Y.-B., Kuo, S.-R. "Impact response of high speed rail bridges and riding comfort of rail cars", *Engineering Structures*, 21(9), pp. 836–844, 1999.
[https://doi.org/10.1016/S0141-0296\(98\)00037-6](https://doi.org/10.1016/S0141-0296(98)00037-6)
- [24] Moliner, E., Lavado, J., Museros, P. "Evaluation of Transverse Impact Factors in Twin-Box Girder Bridges for High-Speed Railways", *Journal of Bridge Engineering*, 21(5), 06016002, 2016.
[https://doi.org/10.1061/\(ASCE\)BE.1943-5592.0000896](https://doi.org/10.1061/(ASCE)BE.1943-5592.0000896)
- [25] Martínez-Rodrigo, M. D., Andersson, A., Pacoste, C., Karoumi, R. "Resonance and cancellation phenomena in two-span continuous beams and its application to railway bridges", *Engineering Structures*, 222, 111103, 2020.
<https://doi.org/10.1016/j.engstruct.2020.111103>
- [26] Liu, K., Su, Q., Ni, P., Zhou, C., Zhao, W., Yue, F. "Evaluation on the dynamic performance of bridge approach backfilled with fibre reinforced lightweight concrete under high-speed train loading", *Computers and Geotechnics*, 104, pp. 42–53, 2018.
<https://doi.org/10.1016/j.compgeo.2018.08.003>
- [27] CEN "EN 1991-2 Eurocode 1: Actions on structures – Part 2: Traffic loads on bridges", European Committee for Standardization, Brussels, Belgium, 2003.
- [28] Galvín, P., Romero, A., Moliner, E., Martínez-Rodrigo, M. D. "Two FE models to analyse the dynamic response of short span simply-supported oblique high-speed railway bridges: Comparison and experimental validation", *Engineering Structures*, 167, pp. 48–64, 2018.
<https://doi.org/10.1016/j.engstruct.2018.03.052>
- [29] Xia, H., Han, Y., Zhang, N., Guo, W. "Dynamic analysis of train–bridge system subjected to non-uniform seismic excitations", *Earthquake engineering & structural dynamics*, 35(12), pp. 1563–1579, 2006.
<https://doi.org/10.1002/eqe.594>
- [30] Lin, C. C., Wang, J. F., Chen, B. L. "Train-induced vibration control of high-speed railway bridges equipped with multiple tuned mass dampers", *Journal of Bridge Engineering*, 10(4), pp. 398–414, 2005.
[https://doi.org/10.1061/\(ASCE\)1084-0702\(2005\)10:4\(398\)](https://doi.org/10.1061/(ASCE)1084-0702(2005)10:4(398))
- [31] Rocha, J. M., Henriques, A. A., Calçada, R. "Safety assessment of a short span railway bridge for high-speed traffic using simulation techniques", *Engineering Structures*, 40, pp. 141–154, 2012.
<https://doi.org/10.1016/j.engstruct.2012.02.024>
- [32] Xia, C. Y., Xia, H., De Roeck, G. "Dynamic response of a train–bridge system under collision loads and running safety evaluation of high-speed trains", *Computers & Structures*, 140, pp. 23–38, 2014.
<https://doi.org/10.1016/j.compstruc.2014.04.010>
- [33] Kwasniewski, L., Li, H., Wekezer, J., Malachowski, J. "Finite element analysis of vehicle–bridge interaction", *Finite Elements in Analysis and Design*, 42(11), pp. 950–959, 2006.
<https://doi.org/10.1016/j.finel.2006.01.014>
- [34] Kwasniewski, L., Wekezer, J., Roufa, G., Li, H., Ducher, J., Malachowski, J. "Experimental Evaluation of Dynamic Effects for a Selected Highway Bridge", *Journal of Performance of Constructed Facilities*, 20(3), pp. 253–260, 2006.
[https://doi.org/10.1061/\(ASCE\)0887-3828\(2006\)20:3\(253\)](https://doi.org/10.1061/(ASCE)0887-3828(2006)20:3(253))
- [35] ORE Committee D23 "Determination of dynamic forces in bridges. Final Report", Office for Research and Experiments of the International Union of Railways, Utrecht, Netherlands, Rep. 17, 1970.
- [36] AREMA "Manual for Railway Engineering", American Railway Engineering and Maintenance-of-way Association, Lanham, MD, USA, 2013.

- [37] UIC "IRS 70778-3: Recommendations for inspection, assessment and maintenance of masonry arch bridges", UIC International Union of Railways, Paris, France, 2017.
- [38] Sarhosis, V., De Santis, S., de Felice, G. "A review of experimental investigations and assessment methods for masonry arch bridges", *Structure and Infrastructure Engineering*, 12, pp. 1439–1464, 2016. <https://doi.org/10.1080/15732479.2015.1136655>
- [39] Panian, R., Yazdani, M. "Estimation of the service load capacity of plain concrete arch bridges using a novel approach: Stress intensity factor", *Structures*, 27, pp. 1521–1534, 2020. <https://doi.org/10.1016/j.istruc.2020.07.055>
- [40] Yazdani, M., Habibi, H. "Residual Capacity Evaluation of Masonry Arch Bridges by Extended Finite Element Method", *Structural Engineering International*, 2021. <https://doi.org/10.1080/10168664.2021.1944454>
- [41] Forgács, T., Sarhosis, V., Bagi, K. "Influence of construction method on the load bearing capacity of skew masonry arches", *Engineering Structures*, 168, pp. 612–627, 2018. <https://doi.org/10.1016/j.engstruct.2018.05.005>
- [42] Yazdani, M. "Three-dimensional Nonlinear Finite Element Analysis for Load-Carrying Capacity Prediction of a Railway Arch Bridge", *International Journal of Civil Engineering*, 19, pp. 823–836, 2021. <https://doi.org/10.1007/s40999-021-00608-w>
- [43] Marefat, M. S., Yazdani, M., Jafari, M. "Seismic assessment of small to medium spans plain concrete arch bridges", *European Journal of Environmental and Civil Engineering*, 23(7), pp. 894–915, 2019. <https://doi.org/10.1080/19648189.2017.1320589>
- [44] Marefat, M.-S., Ghahremani-Gargary, E., Ataei, S. "Load test of a plain concrete arch railway bridge of 20-m span", *Construction and Building Materials*, 18(9), pp. 661–667, 2004. <https://doi.org/10.1016/j.conbuildmat.2004.04.025>
- [45] Mahmoudi Moazam, A., Hasani, N., Yazdani, M. "Three-dimensional modelling for seismic assessment of plain concrete arch bridges", *Proceedings of the Institution of Civil Engineers-Civil Engineering*, 171(3), pp. 135–143, 2018. <https://doi.org/10.1680/jcien.17.00048>
- [46] Bayraktar, A., Altunışık Ahmet, C., Birinci, F., Sevim, B., Türker, T. "Finite-Element Analysis and Vibration Testing of a Two-Span Masonry Arch Bridge", *Journal of Performance of Constructed Facilities*, 24(1), pp. 46–52, 2010. [https://doi.org/10.1061/\(ASCE\)CF.1943-5509.0000060](https://doi.org/10.1061/(ASCE)CF.1943-5509.0000060)